Keto Forms of Salicylaldehyde Schiff Bases: Structural and Theoretical Aspects

Spyros D. Chatziefthimiou, Yannis G. Lazarou, Eugene Hadjoudis, Tereza Dziembowska,† and Irene M. Mavridis*

Institute of Physical Chemistry, National Center for Scientific Research "Demokritos", P.O. Box 60228, Aghia Paraskevi 15310, Greece

Received: June 30, 2006; In Final Form: August 24, 2006

Twelve Schiff bases of methoxy-substituted salicylaldehyde have been examined by crystallographic and spectroscopic methods, as well as by DFT theoretical calculations in order to investigate the effect of the substituent's position on the keto−enol equilibrium in the crystalline state. Four out of the 10 structurally characterized compounds with methoxy substitution on the para and/or ortho positions with respect to the aldimine bridge and deriving from aliphatic amines or alkylarylamines are found as *cis*-keto tautomers and form dimers. In contrast, the five pure enol tautomers derive either from aliphatic or alkylarylamines and are meta substituted or from aniline or benzylamine and are para and/or ortho methoxy substituted. The DFT calculations support the crystallographic results and, moreover, they have shown that keto and enol tautomers are affected differently by the relative arrangement of the monomers. Overall, the DFT calculations point to a plausible hypothesis for the stabilization of the keto form in the crystalline state: In cases with a sufficiently low enol−keto energy difference of the isolated monomers, as when the methoxy group is at ortho and/or para positions with respect to the aldimino group, extra stabilization of the keto form is derived from molecular association, thus leading to its crystallization.

1. Introduction

Schiff bases of salicylaldehyde, *N*-salicylideneamines and particularly *N*-salicylideneanilines (SA), are typical examples of photochromic and thermochromic[1] compounds that continue to attract wide interest because of their technological applications.[1−3] Photochromism and thermochromism of these compounds is due to their ability to undergo proton tautomerism, i.e., reversible change between enol and keto forms caused by electromagnetic radiation or heat. In the case of SAs, photochromism and thermochromism in the crystalline state have been considered as mutually exclusive phenomena.[4−6] Under the accepted Scheme 1, the thermo-product is the *cis*-keto form produced from the enol through intramolecular H-transfer in the ground state, whereas the photoproduct is the *trans*-keto form resulting from the enol by H-transfer in the excited state, subsequent rupture of the intramolecular H-bond and cis−trans isomerization.[1] Because the latter transformation requires a crystal lattice sufficiently "open", planar SAs with dense packing are only thermochromic, whereas nonplanar are photochromic. In the reported crystal structures the molecules are found in the enol-tautomeric form.[1]

However, planarity is not the only factor that affects H-transfer and thus chromobehavior of these compounds. Studies on nonplanar Schiff bases, for example *N*-salicylidenealkylarylamines, which display thermochromism and photochromism simultaneously,[7] suggest that the overall molecular planarity is not a necessary constraint for thermochromism, and it has been postulated that a crucial factor for facile H-transfer resulting in thermochromism is the electron density on the imine N-atom.[8] On the one hand, the latter in *N*-salicylidenealkylarylamines is expected to exhibit increased basicity as compared to the SAs, due to the interruption of conjugation by the alkyl group between the nitrogen lone pair and the aniline ring. On the other hand, increased basicity in planar SAs is due to the fact that their nitrogen lone pair cannot overlap with the π system of the aromatic amine, in contrast to the nonplanar ones. Note, however, that in the *N*-salicylidenealkylarylamines, as in SAs, only the enol tautomers are observed in the crystal structures.[1,7]

Besides the amine part of the molecules, the nature of the substituent group(s) on the salicylidene moiety is a potential factor that can influence the electron distribution of the system and can drive the equilibrium from the phenol-imine toward the keto-amine. However, of the derivatives of simple *N*-salicylideneamines carrying no other H-bonding groups able to affect the enol−keto equilibrium, all exhibit the enol form in the crystalline state,[1,7,9−11] rendering the keto tautomer a rare entity. Two reported cases, *N*-(5-nitrosalicylidene)ethylamine[12] and *N*-(3,5-dichlorosalicylidene)methylamine,[13] probably involving mixtures of keto and enol forms, have been considered as zwitterionic by the authors. Additional functional groups on the salicylidene or the amine moieties that participate in intermolecular interactions have been shown to affect the enol−keto equilibrium as it is found in the Cambridge Structural Database. Thus the presence of a second vicinal hydroxyl group on the salicylidene ring, which participates in intermolecular H-bonding, results in coexistence of the keto-form in significant amounts.[14] Similarly the hydroxy group on the aniline ring of *N*-(5-chlorosalicylide)−4-hydroxyneaniline stabilizes the keto tautomer by intermolecular H-bonding, its effect becoming stronger by decreasing the temperature.[15]

In the present study, we report the spectroscopic and structural characterization of a series of Schiff bases (**1**−**10**) of methoxy-substituted salicylaldehyde (Scheme 2), which carry no ad-

* Corresponding author phone: +30 210 6503793; fax: +30 210 6511766; e-mail: mavridi@chem.demokritos.gr.

† Current address: Institute of Chemistry and Environmental Protection, Technical University of Szczecin Al. Piastów 42, 71−065 Szczecin, Poland.

10.1021/jp064110p CCC: $33.50
Published on Web 11/07/2006

SCHEME 1. Thermochromic and Photochromic Reversible Processes in SA[a]

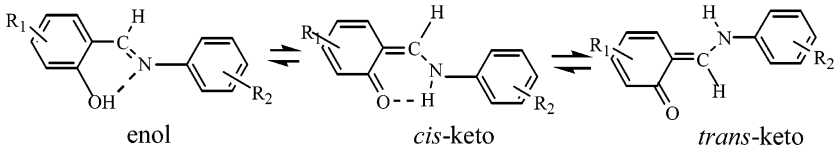

[a] The cis and trans Labelling is Based on the Relative Positions of H (bound to N) Atom with Respect to the Carbonyl O-atom.[4−6]

SCHEME 2: List of the Studied Compounds

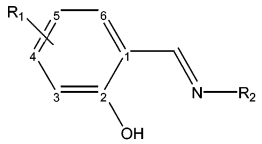

(**1**) R_1= 4-OCH_3, 6-OCH_3, R_2=CH_3
(**2**) R_1= 4-OCH_3, R_2=$(CH_2)_3CH_3$
(**3**) R_1= 4-OCH_3, R_2=$(CH_2)_2$Ph
(**4**) R_1= 4-OCH_3, R_2=CH_3
(**5**) R_1= 4-OCH_3, 6-OCH_3, R_2=CH_2Ph
(**6**) R_1= 4-OCH_3, R_2=Ph
(**7**) R_1= 4-OCH_3, 6-OCH_3, R_2=Ph
(**8**) R_1= 4-OCH_3, R_2=CH_2Ph
(**9**) R_1= 3-OCH_3, R_2=$(CH_2)_2$Ph
(**10**) R_1= 3-OCH_3, R_2=CH_3
(**11**) R_1= 6-OCH_3, R_2=CH_3
(**12**) R_1= 5-OCH_3, R_2=CH_3

ditional groups that may affect the enol−keto equilibrium and/or the molecular packing, four of which are found entirely as the *cis*-keto tautomers (**1**−**4**) in the crystalline state at room temperature. Five bases (**1**, **4**, **10**−**12**) were studied by density functional theory (DFT) calculations in order to understand the role of the methoxy-substitution in the stabilization of the *cis*-keto form. Finally, DFT calculations were also performed for dimers of three derivatives (**1**, **4**, **10**) with various relative arrangements of the monomers in order to gain some insight on the influence of the crystal environment on the equilibrium of the enol and keto forms.

2. Experimental Section

2.1. Syntheses: 4-Methoxy-, 3-methoxy-, 5-methoxy-, and 4,6-dimethoxysalicylaldehydes were purchased from Aldrich Chemicals. Schiff bases were obtained by the standard method of condensation of the substituted salicylaldehydes with the corresponding amines in refluxing ethanol:[16] *N*-(R-salicylidene)−methylamines R = 4,6-di-OCH_3 (**1**), R = 4-OCH_3 (**4**), R = 3-OCH_3 (**10**), R = 5-OCH_3 (**12**) by condensation of respective salicylaldehydes with methylamine;[17] *N*-(4-OCH_3-salicylidene)−butylamine (**2**) by condensation of 4-methoxysalicylaldehyde with butylamine (mp: 43−45 °C); *N*-(4,6-di-OCH_3-salicylidene)-aniline (**7**) by condensation of respective aldehyde with aniline.[18] **3**, $C_{16}H_{17}NO_2$: C, 75.27; H, 6.71; N, 5.49. Found: C, 75.26; H, 6.78; N, 5.50. ^{1}H NMR (500 MHz, [D_6]DMSO, 298 K) δ = 13.92 (s, 1H, −OH), 8.36 (s, 1H, −CH═N-), 7.40−7.20 (m, 6H, Ph, H5), 6.39 (br, dd, J = 8.54 Hz,1H, H6), 6.35 (br, d, 1H, H3), 3.83 (t, J = 7.02 Hz, 2H, −CH2Ph-), 3.79 (s, 3H, −OC*H*3-), 2.98 (t, J = 7.02 Hz, 2H, −NC*H*2-). **5,** $C_{16}H_{17}NO_3$: C, 70.83; H, 6.32; N, 5.16. Found: C, 70.24; H, 6.23; N, 5.11. ^{1}H NMR (500 MHz, [D_6]DMSO, 298 K) δ = 13.49 (s, 1H, −OH), 8.68 (s, 1H, −CH═N-), 7.48−7.28 (m, 5H, Ph), 5.86 (s, 1H, H5), 5.84 (s, 1H, H3), 4.79 (s, 2H, −CH3-), 3.83 (s, 3H, −OC6H3-), 3.78 (s, 3H, −OC4H3). **6.** $C_{14}H_{13}NO_2$: C, 74.00; H, 5.77; N, 6.16. Found: C, 73.89; H, 5.76; N, 6.17.^{1}H NMR (500 MHz, [D_6]DMSO, 298 K) δ = 13.72 (s, 1H, −OH), 8.93 (s, 1H, −CH═N-), 7.59 (d, J = 8.54 Hz, 1H, H5), 7.50 (t, J = 7.63, 2H, H3′, H5′), 7.43 (d, J = 7.93 Hz, 2H, H2′, H6′), 7.33 (t, J = 7.32 Hz, 1H, H4′), 6.62 (br, dd, J = 8.54 Hz, 1H, H6), 6.55 (d, J = 1.53 Hz, 1H, *H*3), 3.87 (s, 3H, −OC*H*3. **8**, $C_{15}H_{15}NO_2$: C, 74.67; H, 6.27; N, 5.80. Found: C, 74.63; H, 6.26; N, 5.82. ^{1}H NMR (500 MHz, [D_6]DMSO, 298 K) δ 13.96 (s, 1H, −OH), 8.62 (s, 1H, −CH═N-), 7.47−7.30 (m, 6H, Ph, H5), 6.48 (br, dd, J = 8.54 Hz,1H, H6), 6.40 (br, d, 1H, H3), 4.79 (s, 1H, −CH2-), 3.80 (s, 3H, −OCH3-). **9**, $C_{16}H_{17}NO_2$: C, 75.27; H, 6.71; N, 5.49. Found: C, 74.80; H, 6.65; N, 5.46. ^{1}H NMR (500 MHz, [D_6]DMSO, 298 K) δ 13.70 (s, 1H, −OH-), 8.49 (s, 1H, −CH═N-), 7.39−7.21 (m, 6H, Ph, H4), 7.02 (dd, J = 7.93 Hz, J = 27.77 Hz, 1H, H6), 6.81 (t, J = 7.63 Hz, 1H, H5), 3.89 (t, J = 6.71 Hz, 2H, −CH2Ph-), 3.81 (s, 3H, −OCH3−), 2.99 (t, J = 7.02 Hz, 2H, −NC).

2.2. Spectroscopic Measurements: The compounds, variations of yellow tint, were screened for photochromic and/or thermochromic properties using thin polycrystalline films. The films were prepared from the melt between two optical quartz plates under pressure and their quality was examined under a polarizing microscope. Absorption spectra were recorded on a JASCO V-5600 spectrophotometer. Steady-state photochemical experiments employed a 200W high-pressure Hg lamp with Corning glass filters. For low-temperature measurements an Oxford cryostat with quartz windows was used.

2.3. X-ray Crystallographic Analysis: Diffraction data of the crystalline compounds **1**−**10** were collected at room temperature with Cu Kα radiation (λ = 1.5418 Å) by the θ-2θ scanning method on a Syntex diffractometer equipped with Rigaku rotating anode and graphite monochromator. The cell dimensions were obtained by least-squares analysis of a number of reflections (20−30) in the range 20° < 2θ < 40°. Three standard reflections, monitored every 97 reflections, showed no decay in intensity during data collection. The data were corrected for Lorentz and polarization effects. X-ray data are summarized in Table 1. The structures were solved by direct methods and refined by full matrix least squares based on F^2 using the program SHELXL97.[19] Anisotropic refinement was applied to all non-hydrogen atoms. Hydrogen atoms were located from the difference Fourier maps. Their coordinates and isotropic thermal parameters were also refined. At the last cycles of refinement all hydrogen atoms, except these bound to O_1, N and C_7, were placed at calculated positions, were assigned Ueq = 1.25U˙eq *o*f the corresponding atom to which they were bonded and they were refined by the riding model. Table 2 contains refinement parameters for all the compounds, one of which, compound **7**, was examined before[13] but it was included in this work for a better evaluation of the enol−keto content. CCDC-296753-296762 contains the supplementary crystallographic data for this paper. These data can be obtained free of charge from The Cambridge Crystallographic Data Center via www.ccdc.cam.ac.uk/data_request/cif.

2.4. DFT Theoretical Calculations: All DFT calculations were performed by using the Gaussian 98 suite,[20] on a Hewlett-

TABLE 1: Details of the Crystal Data of 1−10

compound	empirical formula	space group	a, b, c (Å)	α, β, γ (°)	volume (A^3)	Z, calculated density (mg/m^3)	reflections collected/unique
1	$(C10\ H13\ N\ O3)_2$	$P\bar{1}$	13.333(8) 8.005(5) 9.899(6)	91.59(2) 111.82(2) 90.62(2)	980.2(11)	4, 1.323	2769/2769 [R(int) = 0.0000]
2	C12 H17 N O2	$P2_1/c$	13.234(6) 5.155(2) 16.731(8)	90 92.26(1) 90	1140.5(9)	4, 1.207	1694/1623 [*R*(int) = 0.0192]
3	C16 H17 N O2	$P2_1/c$	15.764(12) 5.796(5) 15.867(11)	90 111.83(2) 90	1345.8(18)	4, 1.260	1979/1908 [*R*(int) = 0.0169]
4	$(C9\ H11\ N\ O2)_2{\cdot}H2O$	$C2/c$	22.915(13) 8.801(6) 19.637(12)	90 110.96(2) 90	3698(4)	8, 1.252	2693/2630 [*R*(int) = 0.0626]
5	C16 H17 N O3	Cc	10.728(8) 22.504(15) 7.861(5)	90.00 132.28(2) 90.00	1404.0(17)	4, 1.284	1963/1003 [*R*(int) = 0.0321]
6	C14 H13 N O2	$C2/c$	23.166(9) 6.171(3) 18.832(8)	90 117.19(1) 90	2394.6(19)	8, 1.261	1735/1695 [*R*(int) = 0.0156]
7	C15 H15 N O3	$P2_1/c$	10.535(4) 9.728(3) 12.755(4)	90 100.656(8) 90	1284.7(7)	4, 1.330	1925/1820 [*R*(int) = 0.0283]
8	C15 H15 N O2	$P2_12_12_1$	5.963(2) 12.993(5) 17.031(6)	90 90 90	1319.5(8)	4, 1.215	1122/1122 [*R*(int) = 0.0000]
9	C16 H17 N O2	$Pna2_1$	23.815(12) 5.067(3) 11.305(6)	90 90 90	1364.1(14)	4, 1.243	1030/1030 [*R*(int) = 0.0000]
10	C9 H11 N O2	Cc	11.497(16) 12.390(17) 6.252(11)	90 93.49(4) 90	889(2)	4, 1.234	633/633 [*R*(int) = 0.0000]

TABLE 2: Crystallographic Structure Refinement for 1−10

	data/restraints/ parameters	goodness-of-fit on F^2	final *R* indices [I > 2 sigma(I)]	*R* indices (all data)	largest diff. peak and hole ($\times A^{-3}$)
1	2769/0/271	1.064	*R*1 = 0.0495 w*R*2 = 0.1503	*R*1 = 0.0528 w*R*2 = 0.1560	0.260 and −0.211
2	1623/0/144	1.178	*R*1 = 0.0478 w*R*2 = 0.1382	*R*1 = 0.0574 w*R*2 = 0.1578	0.388 and −0.476
3	1908/0/181	1.084	*R*1 = 0.0377 w*R*2 = 0.1058	*R*1 =0.0399 w*R*2 = 0.1083	0.159 and −0.123
4	2630/0/251	1.075	*R*1 = 0.0465 w*R*2 = 0.1268	*R*1 = 0.0593 w*R*2 = 0.1391	0.180 and −0.197
5	1003/2/194	1.060	*R*1 = 0.0297 w*R*2 = 0.0793	*R*1 = 0.0332 w*R*2 = 0.0826	0.091and −0.134
6	1695/0/164	1.143	*R*1 = 0.0378 w*R*2 = 0.1115	*R*1 = 0.0414 w*R*2 = 0.1154	0.101 and −0.139
7	1820/0/181	1.056	*R*1 = 0.0457 w*R*2 = 0.1235	*R*1 = 0.0503 w*R*2 = 0.1287	0.304 and −0.200
8	1122/1/173	1.083	*R*1 = 0.0414 w*R*2 = 0.1122	*R*1 = 0.0536 w*R*2 = 0.1237	0.141 and −0.102
9	1030/1/181	1.067	*R*1 = 0.0345 w*R*2 = 0.0835	*R*1 = 0.0550 w*R*2 = 0.0957	0.100 and −0.114
10	633/2/117	1.088	*R*1 = 0.0317 w*R*2 = 0.0877	*R*1 = 0.0346 w*R*2 = 0.0912	0.096 and −0.109

Packard mainframe computer running HP-UX. The B3P86[21,22] and B3LYP[21,23] functionals were employed in conjunction with the cc-pVDZ, aug-cc-pVDZ, and aug-cc-pVTZ correlation-consistent basis sets of Dunning.[24]

SCHEME 3. Atom Numbering Scheme for the Salicylaldimine(amine) Groups

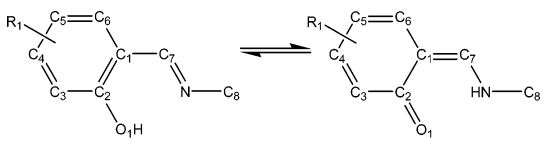

3. Results and Discussion

3.1. Crystal and Molecular Structures: According to our results of the 10 examined molecules (Scheme 2), four are found in the keto form (**1**−**4**), one is an equimolar mixture of keto and enol forms (**5**, roughly 50%), and five are found in the enol-form (**6**−**10**). The keto group of molecules has the methoxy substituent(s) on the 4- or 4,6-(para or para and ortho position-(s) with respect to the aldimine bridge) (Scheme 3). The amine parts are methylamine (**1**, **4**), butylamine (**2**), or 2-phenylethylamine (**3**). The enol group comprises five enol tautomers with methoxy substitution (i) at position 3- (meta) that derive from either aliphatic or alkylarylamines (**10**, **9**); (ii) at position 4-deriving from aniline or benzylamine (**6**, **8**); and (iii) at positions 4,6-, deriving from aniline (**7**). It is interesting to note that **5**, which is a 1:1 mixture of keto and enol tautomers, differs from

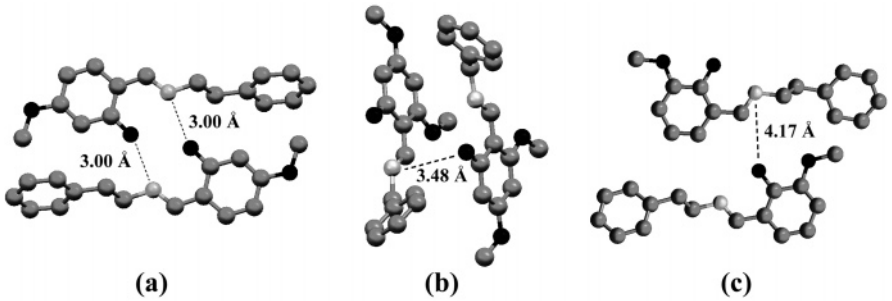

Figure 1. Intermolecular associations (with O···N distances) of (a) a characteristic dimer of the keto group (**3**); (b) **5**, a mixture of enol and keto forms; (c) a dimer of the enol group (**9**). Color code: O-atoms, black; C-atoms, gray; N-atom: light gray).

TABLE 3: Characteristic Bond Lengths (Å) of the Crystallographically Examined Compounds, 1−10, with Standard Deviations in Parentheses

bond	**1**	**2**	**3**	**4**	**5**	**6**	**7**	**8**	**9**	**10**
C_1-C_2	1.442(3)	1.437(3)	1.437(2)	1.440(3)	1.429(4)	1.404(2)	1.411(3)	1.409(5)	1.395(6)	1.392(4)
C_1-C_6	1.430(3)	1.407(3)	1.406(2)	1.412(3)	1.432(4)	1.403(2)	1.408(3)	1.391(5)	1.389(6)	1.403(5)
C_2-C_3	1.429(3)	1.425(3)	1.425(2)	1.421(3)	1.412(4)	1.385(2)	1.373(3)	1.385(4)	1.398(5)	1.403(5)
C_3-C_4	1.357(3)	1.360(3)	1.360(2)	1.371(3)	1.370(4)	1.382(2)	1.379(3)	1.379(4)	1.376(6)	1.373(5)
C_4-C_5	1.417(3)	1.410(3)	1.406(2)	1.413(3)	1.404(4)	1.391(3)	1.390(3)	1.380(5)	1.389(7)	1.389(6)
C_5-C_6	1.363(3)	1.357(3)	1.359(2)	1.358(3)	1.368(4)	1.363(3)	1.382(3)	1.352(5)	1.366(6)	1.364(6)
C_1-C_7	1.396(3)	1.409(3)	1.410(2)	1.410(3)	1.413(4)	1.442(2)	1.434(3)	1.446(5)	1.463(6)	1.459(5)
C_2-O_1	1.268(2)	1.268(2)	1.271(2)	1.283(3)	1.293(4)	1.350(2)	1.349(2)	1.347(4)	1.340(5)	1.351(4)
C_7-N	1.299(2)	1.294(3)	1.293(2)	1.298(3)	1.294(4)	1.286(2)	1.280(3)	1.264(5)	1.268(5)	1.264(5)
C_8-N	1.452(2)	1.452(2)	1.453(2)	1.457(3)	1.455(4)	1.414(2)	1.417(3)	1.464(5)	1.462(5)	1.451(5)
$C_{4\text{ or }3}-O_2$	1.365(2)	1.366(2)	1.364(2)	1.365(3)	1.368(4)	1.362(2)	1.359(2)	1.363(4)	1.377(5)	1.363(4)
C_6-O_3	1.361(2)	- - -	- - -	- - -	1.355(3)	- - -	1.359(2)	- - -	- - -	- - -

TABLE 4: Intramolecular H-bonds and Average Intermolecular Distance O···N

	intramolecular H-bond ($O_1-H\cdots N$ or $O_1\cdots H$-N) distances (Å) and angles (degrees)					average intermolecular $O_1\cdots H$-N distances (Å)		
compound	$O_1\cdots N$	$H_{OH}\cdots N$	O_1-H···N	$O_1\cdots H_N$	O_1... H-N	$O_1\cdots N$	$O_1\cdots H_N$ or $N\cdots H_{OH}$	tautomeric percentage
1	2.644			1.981	128.8	2.934	2.206	100% keto
2	2.642			1.984	133.3	2.949	2.284	100% keto
3	2.615			1.858	136.0	3.004	2.316	100% keto
4	2.630			1.882	130.0	3.065	2.302	100% keto
5	2.552	1.759	137.8	1.870	146.2	3.478	3.693/3.668	50% enol
6	2.580	1.674	155.9			3.539	4.084	100% enol
7	2.595	1.708	153.2			5.416	6.364	100% enol
8	2.607	1.758	142.0			4.394	4.572	100% enol
9	2.569	1.746	158.1			4.169	4.571	100% enol
10	2.590	1.745	149.3			4.575	5.163	100% enol

7 (a SA in enol form) in that the phenyl group is displaced by a methylene group from the nitrogen atom. The same relation exists between **3** (100% keto) and **8** (100% enol). In general, it is difficult to correlate both the substituent effect and the nature of the amine with the tautomeric equilibrium in the solid-state, because the latter may result from concerted electronic and steric interactions operating simultaneously in the intra- and intermolecular level. Nevertheless, the present results indicate that methoxy derivatives substituted at the 4- or 4,6-position(s) derived from aliphatic amines exist as keto tautomers, whereas methoxy derivatives substituted at the 3-position exist as enol tautomers. If the amine contains an aryl group directly bound to the N-atom, the keto-stabilizing effect of the methoxy groups at the 4- or 4,6-positions is canceled. If one methylene group intervenes between the nitrogen and the phenyl carbon atoms, substitutions at both 4- and 6-positions offer some stabilization of the keto form (**5**), whereas substitution only at 4-position, does not (**8**). If two methylene groups intervene between the nitrogen and the phenyl carbon atoms, even single substitution at position 4- results in a keto compound (**3**).

The percentage of the keto/enol ratio was calculated from the relative intensity of the electron density of the hydroxyl and/or amine H-atom, whose position was determined from the difference Fourier maps after all the other hydrogen atoms had been located (Supporting Information Figure S1) and was further verified by least squares refinement of their occupancies. Comparison of bond lengths (Table 3) reveals differences reflecting their keto or enol character to a sufficient extent: The C_2-O_1 and C_7-N lengths (1.340−1.351 and 1.264−1.286 Å, respectively) of the enol compounds **6**−**10** (Scheme 3) have the typical values of SAs in the enol form.[10] In contrast, the corresponding bond lengths (1.268−1.283 and 1.293−1.299 Å) of the keto compounds **1**−**4** approach the values of C═O and C−N bond lengths of quinones and enamines, 1.222 and 1.339 Å, respectively. Additional characteristic differences between the keto and enol categories are exhibited in the C_1-C_2 and C_1-C_7 lengths, i.e., in the keto category; C_1-C_2 (1.437−1.442 Å) deviates appreciably from the aromatic bond length, whereas C_1-C_7 (1.396−1.410 Å) approaches it. The keto character becomes also apparent in the alternating long−short bond length trend of the salicylic ring (Table 3), an indication of deviation from aromaticity. The bond distances reported for *N*-(3,5-dichlorosalicylidene) methylamine[13] lie between the values of the keto category and **5** (an equimolar mixture of keto and enol

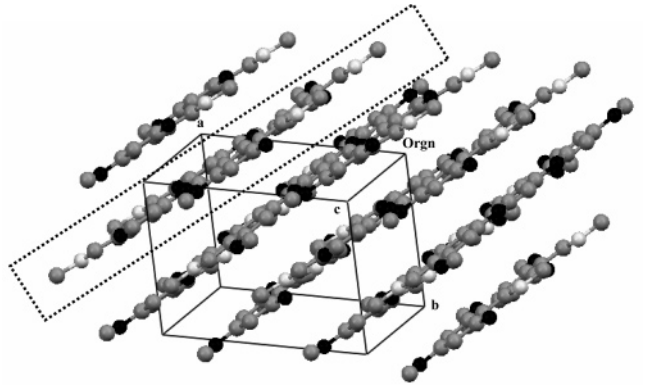

Figure 2. Layers in the crystal lattice of **1**, where each layer contains the coplanar dimers (color code as in Figure 1).

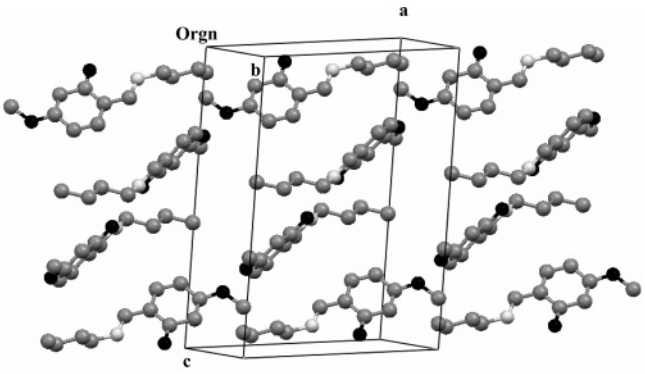

Figure 3. Bilayers in the crystal lattice of **2** along the **ab** plane. The salicylidene rings of the dimers are coplanar within the bilayers (color code as in Figure 1).

forms). The salicylalideneimine(amine) moieties of **1**−**10** are planar (Supporting Information Table S1), the nitrogen atom and the accompanying H_N of **1**−**4** showing the highest deviations from the least-squares plane of the aromatic ring atoms.

Although the examined molecules do not pack in a unique way, similar packing characteristics are shared within the keto and enol groups. The keto group molecules associate in pairs via mutual O···H−N intermolecular H bonds (O···N distances, 2.93−3.06 Å) forming dimers (Figure 1a,[25] Table 4), whereas no dimers are formed in the enol group or **5**. The monomers comprising the dimers lie in the same layer in the crystal lattice, as in **1** (Figure 2), or in different layers, as in **2**, **3** (Figure 3). In the latter case, the interacting molecules form bilayers. In both cases, the salicylidene rings of the dimers are nearly coplanar (Supporting Information Table S1, last column). In contrast to the keto dimers, the O···N distances between the nearest monomers of the remaining compounds are longer (3.54−5.42 Å) (Table 4 and Figure 1b,c) and the hydroxyl hydrogen atom does not point toward the nitrogen atom. Only two cases of $\pi-\pi$ interactions are observed in the crystal lattices, namely in **1**, (between the methoxy groups and the salicylaldimine groups) and in **7** (Supporting Information Figure S2).

A different kind of intermolecular dimer is observed in **4**, which cocrystallized with one molecule of water (Figure 4). The keto oxygen atoms (O_1) of two neighboring molecules form two strong hydrogen bonds with the two hydrogen atoms of the water molecule. The bond lengths of **4** are very similar to those of **1**−**3**; especially **2** and **3**, which have exactly the same substitution on the salicylic moiety as **4** (Table 3). Therefore, since the existence of 100% keto tautomer in **4** was determined quite accurately, because it was based not only on the location of the hydrogen atom (on the amine) but on the presence of one molecule of water as well, it is confirmed that **1**−**3** are also found in the keto form.

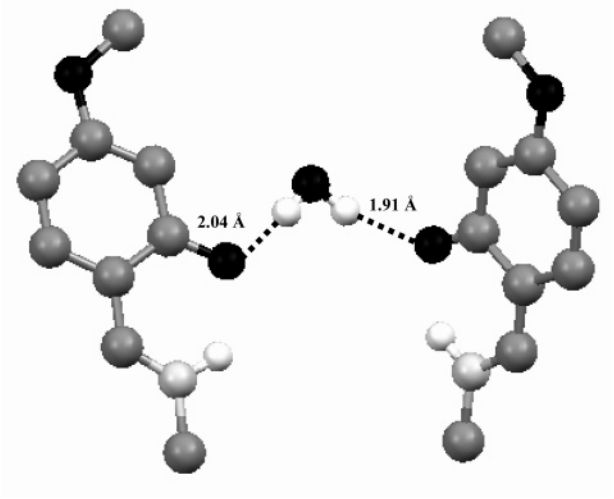

Figure 4. Hydrogen bonds between the keto-oxygen atoms (O_1) of two monomers of **4** and the cocrystallized water molecule (H-atoms (white) only on N-atoms and the water molecule, color code as in Figure 1).

TABLE 5: Photochromic (P) and/or Thermochromic (T) Behavior of Compounds 1−10, 12

compound	**1**	**2**	**3**	**4**	**5**	**6**	**7**	**8**	**9**	**10**	**12**
chromo behavior	P/T	P/T	P/T		P/T	P	T	P/T	P/T	P/T	P/T

Additional differences between the examined keto and enol groups of molecules are the intramolecular H-bond distances (Table 4). The $H_{O1}\cdots N$ distances of the enol compounds are shorter than the $O_1\cdots H_N$ distances of the keto, alluding to stronger intramolecular H-bonds for the former. This is supported by the shorter $O_1\cdots N$ distances and higher values of $O_1\cdots H\cdots N$ angles in the enol category (**6**−**10**).

3.2. Photochromic and Thermochromic Behavior: The spectral variations with temperature and ultraviolet irradiation (365 nm) of polycrystalline thin films and powders of the Schiff bases **1**−**10** and **12** were studied at room and liquid nitrogen temperature (Table 5). At room temperature, the thermochromic compounds exhibit an absorption band ranging from 400 to 440 nm (Supporting Information Figure S3), attributed to the *cis*-keto form, which is slightly attenuated on cooling to liquid nitrogen temperature. None of the compounds shows thermochromic behavior upon heating above room temperature. In the case of photochromic compounds, ultraviolet irradiation at liquid nitrogen temperature leads to the appearance of a weak absorption band, attributed to the *trans*-keto form, positioned either in the same region as the thermochromic band or displaced to longer wavelengths. No photochromic behavior has been observed at room temperature. Of the compounds in this study, only **6** and **7** are Schiff bases of aromatic amines (SA) and, as expected, they are typically either thermochromic (**7**) or photochromic (**6**). The photochromic and/or thermochromic properties of the compounds are weak, their strength in increasing order being (**1**, **2**, **10**, **12**) < (**3**, **9**) < (**5**, **8**) < (**6**, **7**). The weakest properties are shown by the *N*-salicylidenealkylamines, followed by the *N*-salicylidenealkylarylamines and finally by the *N*-salicylideneanilines. Compound **4**, cocrystallized with one molecule of water and locked in the keto form, does not show thermochromism, because it cannot participate in the tautomeric equilibrium of Scheme 1. It does not show photocromism either, because the latter is due to the excitation of the enol form.[26,27] The position of the methoxy group on the

salicylic ring does not affect the strength of thermochromic behavior, since **1** and **2** (keto form) are as weakly thermochromic as **10** and **12** (enol form). The decreased photochromic efficiency of the methoxy substituted N-salicylidenealkylamines, in comparison to SAs, may stem from the influence of the substituent on the relative energies of the π,π^* and n,π^* electronic states. It is believed that the relative positions of the energy levels of the above excited states are sensitive to the substituent groups, as well as to hydrogen bonding.[28,29] The n,π^* state leads to photoreaction, thus if its energy is very close to that of the π,π^* state, the efficiency of photochromism decreases, whereas if its energy is higher, no photochromism is observed.

3.3. DFT Theoretical Calculations: The crystallographic study of compounds **1**−**10** indicates that the stabilization of the keto or enol tautomeric form in the crystalline state is a function of the position of the methoxy group on the salicylidene moiety. To understand the crystallographic results and to distinguish between the effects of (i) the position of the methoxy group in the isolated molecule and (ii) the role that intermolecular interactions play in stabilizing the keto form in the crystalline state, DFT calculations[30] were carried out for **1**, **4**, **10**, **11**, and **12** (Scheme 2). The first effect was evaluated by calculations on isolated molecules and the second by calculations on dimers with relative arrangements suggested by the observed crystal structures. Only Schiff bases of methylamine were included in the DFT computations, because of the exceedingly large computational resources required for larger molecules. Initially, full geometry optimizations and vibrational frequency calculations at the B3P86/cc-pVDZ and B3LYP/cc-pVDZ levels of theory were performed for the isolated molecules at their most important conformations (*syn*-enol, *anti*-enol, *cis*-keto, and two *trans*-keto isomers), shown in Figure 5[31] for **1**. In all cases, the absence of imaginary harmonic frequencies shows that the optimized structures correspond to true minima in the potential energy surface. The most stable structures for all compounds considered are the *syn*-enol and the *cis*-keto, followed by the *anti*-enol and the *trans*-keto forms. The variations in optimized bond lengths between the two functionals employed were negligible, with an average deviation of 0.003 Å for all structures of each molecule. The mean absolute differences between the calculated and crystallographic bond lengths are small, 0.013 Å, (Table 6) and they follow the same trend. Further refinement of the electronic energies was based on molecular structures optimized at the B3P86/cc-pVDZ level of theory, since the B3P86 functional has been shown to be better than B3LYP in geometry optimizations.[32]

Total energies were improved by single point calculations employing the extended basis set, aug-cc-pVTZ, with both the B3P86 and B3LYP functionals, for the *syn*-enol (enol form) and *cis*-keto (keto form). The enol form was found to be energetically the most stable tautomer, for **4**, **10**, **11**, and **12** (Table 7) at all levels of theory but not for **1**. However, although the enol-keto energy difference for **10** and **12** (methoxy substitution at positions 3- or 5, respectively) does not change appreciably by improving the quality of the calculation, this difference progressively diminishes for **1**, **4**, and **11** (methoxy substitution at positions 4,6-, 4-, or 6-, respectively). Thus, at the highest levels of theory, the energy difference between the enol and keto forms of **10** and **12** is 15.3 and 18.0 kJ/mol, respectively (average values from Table 7 for the two functionals giving almost identical predictions), whereas it drops to 10.8 and 11.7 kJ/mol for **4** and **11,** respectively, and approaches zero for **1** (Table 7). Indeed, the keto form is found to be the most

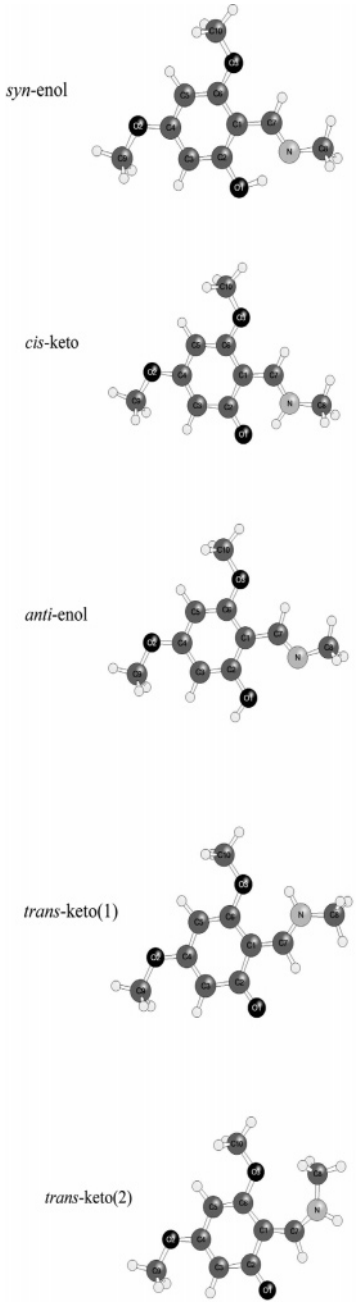

Figure 5. The conformations of **1** considered in the DFT calculations.

stable tautomer for **1** at the B3LYP/aug-cc-pVTZ level of theory (Table 7). The decrease of the energy difference between enol and keto forms suggests that in the isolated molecule substitution of the methoxy group at ortho and/or para positions with respect to the aldimine group plays an important role in the stabilization of the keto form. The effect of the methoxy group can be explained in terms of an effective electron density transfer to the nitrogen atom through conjugation. This transfer is reflected in a systematic increase of the Mulliken electron density on the nitrogen atom of the enol form for **1**, **4,** and **11**, followed by a corresponding decrease of the electron density on the oxygen atom of the hydroxyl group and on the oxygen and carbon atom of the methoxy group. However, the decrease of the electron density on the methoxy group is less systematic, due to the electronic effects of the neighboring groups, especially the hydroxyl. The combination of the above effects leads to an increased basicity of the nitrogen atom and a gain in the stabilization of the keto form for the methoxy derivatives at

TABLE 6: Selected Geometrical Parameters Determined by DFT Calculation (B3P86/cc-pVDZ) and X-ray Crystallography for Three of the Studied Compounds (1, 4, 10)

	1		**4**		**10**	
bond	crystal data (Å)	calculated keto-	crystal data (Å)	calculated keto-	crystal data (Å)	calculated enol-
C_1-C_2	1.442	1.461	1.440	1.460	1.392	1.413
C_1-C_6	1.430	1.432	1.412	1.421	1.403	1.411
C_2-C_3	1.429	1.431	1.421	1.433	1.403	1.420
C_3-C_4	1.357	1.377	1.371	1.379	1.373	1.389
C_4-C_5	1.417	1.426	1.413	1.429	1.389	1.406
C_5-C_6	1.363	1.373	1.358	1.366	1.364	1.380
C_1-C_7	1.396	1.398	1.410	1.401	1.459	1.449
C_2-O_1	1.268	1.267	1.283	1.268	1.351	1.329
C_7-N	1.299	1.319	1.298	1.318	1.264	1.285
C_8-N	1.452	1.437	1.457	1.436	1.451	1.440
$C_{(4\text{ or }3)}-O_2$	1.365	1.353	1.365	1.352	1.363	1.355
C_6-O_3	1.361	1.357	---	---	---	---

TABLE 7: Energy Differences ΔE_0 (Including Zero-Point Energies) Between the Enol and Keto Forms

	ΔE_0 (kJ/mol)				
level of theory	**1**	**4**	**10**	**11**	**12**
B3P86/cc-pVDZ	−8.9	−13.2	−15.9	−13.1	−18.1
B3LYP/cc-pVDZ	−9.4	−14.6	−17.5	−14.6	−20.2
B3P86/aug-cc-pVDZ	−6.2	−10.6	−14.2		
B3LYP/aug-cc-pVDZ	−5.3	−10.6	−14.6		
B3P86/aug-cc-pVTZ	−5.5	−11.0	−15.3	−11.9	−17.9
B3LYP/aug-cc-pVTZ	4.3	−10.6	−15.3	−11.5	−18.1

positions 4- and/or 6-. The conjugative effects are also reflected in the pattern of C−C bond lengths within the salicylic ring with alternating long and short distances, most notably for the calculated keto forms, suggesting a decreased aromatic character. By the same reasoning, the keto character in *N*-(5-nitrosalicylidene)ethylamine[12] and *N*-(3,5-dichlorosalicylidene)methylamine[13] may be attributed to the increased acidity of the hydroxylic hydrogen atom as a result of the electron attracting nitro group and chlorine atoms at positions ortho and/or para to the hydroxyl group, respectively.

The role of intermolecular interactions developing during the crystallization process was investigated by calculating the absolute electronic energies of dimers of **1**, **4**, and **10**. The geometrical parameters obtained from the B3P86/cc-pVDZ calculations were used for the individual molecules in the dimers considered separately as enol and keto tautomers. As relative arrangements of the two monomers, those possessing the closest intermolecular O···N distance in the crystalline state were used, thus they are denoted as dimer-**1** and dimer-**4** if they are arranged as in the crystals of **1** and **4** and dimer-**10a** and dimer-**10b** if arranged as in **10** (two close orientations exist in the crystal, both exhibiting O···N distances of 4.6 Å). In the above arrangements the following hypothetical dimers (not observed in the crystals) have been included in addition to those observed in the crystals:

(a) For **1** and **4**, dimers in two orientations, namely those that the molecules would have if the packing were that of **10 (**dimer-**10a** and dimer-**10b**).

(b) For **10**, dimers in two hypothetical "H-bond forming" orientations, namely those that the molecules would have if the packing were as in **1** and **4 (**dimer-**1** and dimer-**4**, respectively).

(c) Finally, for **4**, an additional hypothetical "H-bond forming" orientation, namely the one the molecules would have if the packing were as in **1** (dimer-**1**). The latter corresponds to closer intermolecular distances than those observed in the crystals of **4**.

The electronic energies of all dimers were calculated at the B3P86/aug-cc-pVDZ and B3LYP/aug-cc-pVDZ levels of theory.

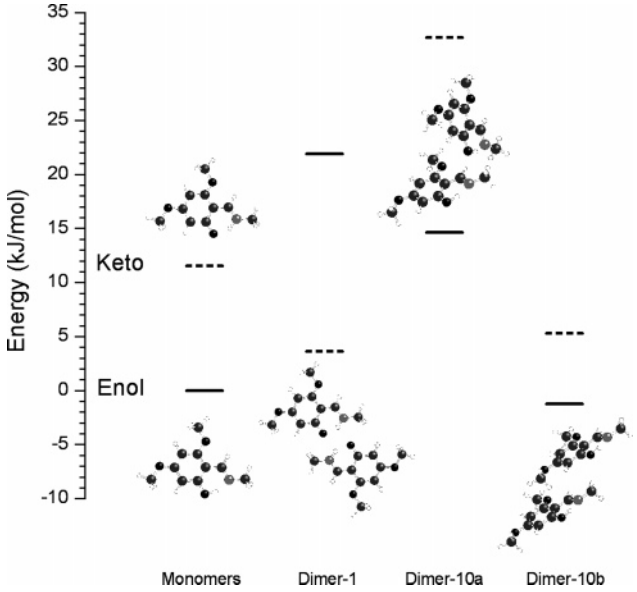

Figure 6. Relative electronic energies at the B3LYP/aug-cc-pVDZ level of theory for the enol- and keto-forms (full and dashed lines, respectively) for three different arrangements of the dimers of **1**, with respect to the energies of a pair of noninteracting *syn*-enol or *cis*-keto monomers.

The relative energies at the B3LYP/aug-cc-pVDZ level for the above relative arrangements of the enol and keto dimers, with respect to the sum of the energies of two monomers are shown in Figures 6, 7, and 8, for **1**, **4,** and **10**, respectively. It is predicted that the keto dimer-**1** of **1** (Figure 6), which corresponds to the one found in the crystalline state, is stabilized, considerably, with respect to the two individual keto monomers, whereas that of the enol is destabilized. The net result is that keto dimer-**1** is more stable than enol-dimer-**1**. Enol dimers **10a** and **10b** of **10** (as found in the crystalline state) are stabilized **(**Figure 8), albeit less than the keto dimers. Thus although the enol dimers-**10a** and **10b** of **10** are predicted to be the most stable, their energy difference from the corresponding keto (with respect to monomers) decreases. The case of **4** is very similar to that of **1** (Figure 7), even for the additional hypothetical orientation (dimer-**1**) that brings the molecules closer than in the crystal and in coplanar fashion.

In general, it can be seen that the keto dimers (even the hypothetical ones) are preferentially stabilized in all the relative arrangements of monomers considered (an exception to the above is dimer-**10a** of **1**, where both keto- and enol-forms are destabilized because of nonbonding repulsions due to the methoxy group at position 6-). In contrast, the enol dimers are

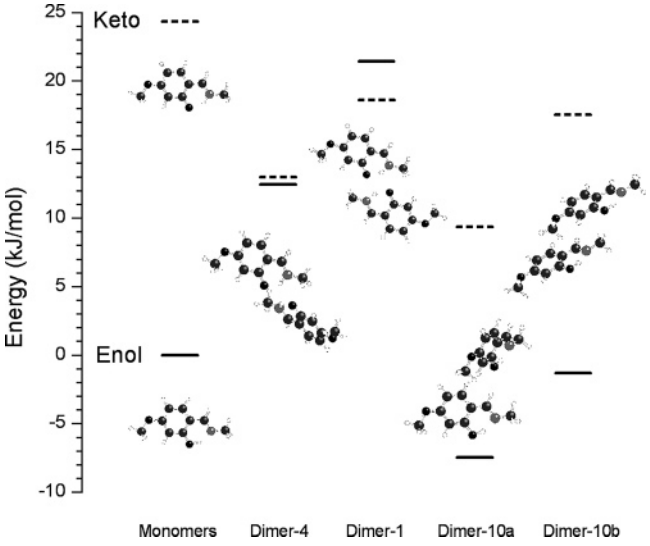

Figure 7. Relative electronic energies at the B3LYP/aug-cc-pVDZ level of theory for the enol- and keto-forms (full and dashed lines, respectively) for four different arrangements of the dimers of **4**, with respect to the energies of a pair of noninteracting *syn*-enol or *cis*-keto monomers.

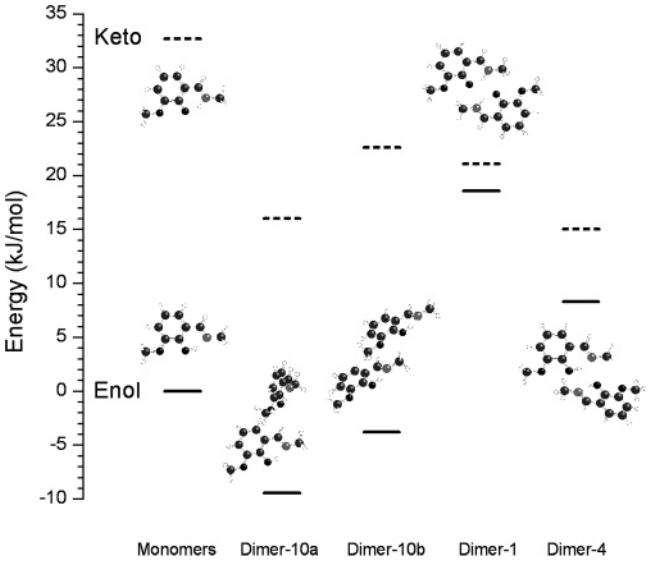

Figure 8. Relative electronic energies at the B3LYP/aug-cc-pVDZ level of theory for the enol- and keto-forms (full and dashed lines, respectively) for four different arrangements of the dimers of **10**, with respect to the energies of a pair of noninteracting *syn*-enol or *cis*-keto monomers.

stabilized only for relative arrangements and distances between monomers as they appear in the crystal of **10**, but even in this case, the stabilization is less than that of the keto dimers. For the orientations which bring the O···N atoms of two monomers sufficiently close (denoted as dimer-**1** and dimer-**4**), examination of the geometrical parameters reveals that the keto dimers possess shorter intermolecular $O_1 \cdots H_N$ distances by 0.08 Å than the $H_{O1} \cdots N$ distances for the corresponding enol dimers. In addition, keto-dimers possess weaker nonbonding repulsions due to longer intermolecular $H_N \cdots H_N$ distances by about 0.25 Å as compared to the $H_{O1} \cdots H_{O1}$ distances for the enol dimers. It should be stressed that the above results of the relative energies of the dimers do not change appreciably when the electronic energies are calculated at the B3P86/aug-cc-pVDZ level of theory (Supporting Information Table S2), suggesting that the energetics of the various arrangements of the dimers (computed by using either B3LYP or B3P86 functionals) can be considered to be sufficiently accurate.

Overall, the DFT theoretical calculations point to a plausible hypothesis for the stabilization of the keto form in the crystalline state of the examined compounds. Although in the isolated monomers the enol form is more stable than the keto form, in cases with a sufficiently low enol-keto energy difference, as in **1** and **4**, extra stabilization of the keto form can be derived from molecular association due to the molecular packing, which leads to the crystallization of the keto form.

4. Conclusions

The X-ray crystallographic study of ten Schiff bases of methoxy substituted salicylaldehydes, that carry no additional functional groups that may affect the enol−keto equilibrium and the molecular packing, has revealed compounds crystallized as *cis*-keto tautomers, in contrast to previous cases, for which enol form crystallization was the rule. The observed differentiation is a function of the position of the methoxy group and the nature of the amine part of the molecule. DFT theoretical calculations on five derivatives (**1**, **4**, **10**, **11**, and **12**) of *N*-salicylidenemethylamine attempt to isolate the electronic effect of the methoxy substitution in the salicylidene ring from the steric and other interactions of the amine moiety. Indeed, the position of the methoxy group influences the relative energies of the enol vs the keto tautomers, substitution on the 4- or 4,6- (para or ortho and para) positions with respect to the aldimine bridge stabilizing the keto-form (**1**, **4**, and **11**). This agrees with the crystallographic results, which show that the keto group molecules have methoxy substitution at the 4- or 4,6- positions and derive from methylamine (**1**, **4**), butylamine (**2**) or 2-phenylethylamine (**3**). The enol compounds, on the other hand, have methoxy substitution at (i) position 3- (meta) and derive from aliphatic or alkylarylamines (**9**, **10**), (ii) position 4- deriving from aniline or benzylamine (**6**, **8**), (iii) positions 4,6-, deriving from aniline (**7**). Thus our study indicates that *N*-(4- or 4,6-methoxysalicylidene)alkylamines crystallize as keto tautomers, whereas the corresponding compounds substituted at the 3-position crystallize as enol tautomers. In the case of the 4- or 4,6-methoxy derivatives, if the amine contains an aryl group, the existence and length of the alkyl may favor one form or the other. If the aryl group is directly bound to the N-atom the stabilizing effect of the methoxy groups is canceled. If one methylene group intervenes between the nitrogen and the phenyl carbon atoms, substitution at 4- and 6- positions offers some stabilization of the keto form and if two methylene groups intervene, keto compounds result.

The crystal structures indicate that the bond lengths reflect the keto or enol character of the compounds. This is in agreement with the optimized geometry by DFT calculations. The crystal structures reveal also that the keto group molecules associate in pairs through O···H−N intermolecular H-bonds, with their salicylideamine moieties coplanar, forming layers or bilayers. Dimer formation is not observed in the enol group. The intermolecular associations in the crystalline state correlate well with the predictions of DFT calculations on dimers of three compounds (**1**, **4,** keto-form and **10,** enol-form), which reveal different behavior for the dimers of the enol and keto forms. Thus, enol dimers of all compounds are stabilized only when the monomers are arranged as in the crystals of the enol molecule, in which no O−H···N intermolecular association exists. In contrast, the keto dimers are stabilized for all relative arrangements of the two monomers and their stabilization is greater than that of the enol (when it is predicted). By

considering energetic and structural data on the above dimers, it can be proposed that intermolecular interactions of keto dimers contribute to their stability, whereas the enol form is favored by weaker interactions. Therefore, if the energy levels of the enol and the keto monomers are sufficiently close, as in **1** and **4 (**substituted by methoxy groups in the 4- or 4,6- positions), the keto dimers are further stabilized by close intermolecular association, which in turn, favors their formation and by extrapolation it leads to their crystallization.

Acknowledgment. The support of Empirikion Foundation (I.M.M.), as well as the scholarship by NCSR Demokritos (S.D.C.) are kindly acknowledged.

Supporting Information Available: Two tables and three figures containing further details of the analysis. This material is available free of charge via the Internet at http://pubs.acs.org.

References and Notes

(1) Hadjoudis, E.; Mavridis, I. M. *Chem. Soc. Rev.* **2004**, *33*, 579.

(2) Feringa, B. L.; Jager, W. F.; deLange, B. *Tetrahedron* **1993**, *37*, 8267.

(3) Amimoto, K.; Kawato, T. *J. Photochem. Photobiol. C: Photochem. Rev.* **2005**, *6*, 207−226.

(4) Cohen, M. D.; Schmidt, G. M. J. *J. Phys. Chem.* **1962**, *66*, 2442.

(5) Bregman, J.; Leiserowitz, L.; Osaki, K. *J. Chem. Soc.* **1964**, 2086.

(6) Bregman, J.; Leiserowitz, L.; Schmidt, G. M. J. *J. Chem. Soc.* **1964**, 2068.

(7) Hadjoudis, E.; Vittorakis, M.; Moustakali-Mavridis, I. *Tetrahedron* **1987**, *43*, 1345.

(8) Hadjoudis, E. Tautomerism by hydrogen transfer in anils. In *Photochromism: Molecules and Systems*; Durr, H., Bouas-Laurent, H., Eds.; Elsevier: Amsterdam, 1990; pp 685 and references therein.

(9) Schmidt, G. M. J. *Reactivity of The Photoexcited Organic Molecule*; Interscience: New York, 1967.

(10) Moustakali-Mavridis, I.; Hadjoudis, E.; Mavridis, A. *Acta Crystallogr.* **1978**, *B34*, 3709.

(11) Hadjoudis, E.; Rontoyianni, A.; Ambroziak, K.; Dziembowska, T.; Mavridis, I. M. *J. Photochem. Photobiol. A: Chem.* **2004**, *162*, 521.

(12) Krygowski, T. M.; Wozniak, K.; Anulewicz, R.; Pawlak, D.; Kolodziejski, W.; Grech, E.; Szady, A. *J. Phys. Chem.* **1997**, *101*, 9399.

(13) Filarowski, A.; Koll, A.; Glowiak, T.; Majewski, E.; Dziembowska, T. *Ber. Bunsen-Ges. Phys. Chem.* **1998**, *102*, 393.

(14) Mansilla-Koblavi, F.; Tenon, J. A.; Toure, S.; Ebby, N. D.; Lapasset, J.; Carles, M. *Acta Crystallogr.* **1995**, *C51*, 1595.

(15) Ogawa, K.; Kasahara, Y.; Ohtani, Y.; Harada, J. *J. Am. Chem. Soc.* **1998**, *120*, 7107.

(16) Furnuss, B. S.; Smith, A. J. H.; P. W.; Tatchell, A. *Textbook of Practical Organic Chemistry*; Longmans: New York, 1989.

(17) Rozwadowski, Z.; Majewski, E.; Dziembowska, T.; Hansen, P. E. *J. Chem. Soc., Perkin Trans. 2* **1999**, 2809.

(18) Krygowski, T. M.; Stepien, B.; Anulewicz-Ostrowska, R.; Dziembowska, T. *Tetrahedron* **1999**, *55*, 5457.

(19) Sheldrick, G. M. SHELXL97; University of Goettingen: Goettingen, Germany, 1997.

(20) Frisch, M. J.; Trucks, G. W.; Schlegel, H. B.; Scuseria, G. E.; Robb, M. A.; Cheeseman, J. R.; Zakrzewski, V. G.; Montgomery, J. A., Jr.; Stratmann, R. E.; Burant, J. C.; Dapprich, S.; Millam, J. M.; Daniels, A. D.; Kudin, K. N.; Strain, M. C.; Farkas, O.; Tomasi, J.; Barone, V.; Cossi, M.; Cammi, R.; Mennucci, B.; Pomelli, C.; Adamo, C.; Clifford, S.; Ochterski, J.; Petersson, G. A.; Ayala, P. Y.; Cui, Q.; Morokuma, K.; Malick, D. K.; Rabuck, A. D.; Raghavachari, K.; Foresman, J. B.; Cioslowski, J.; Ortiz, J. V.; Stefanov, B. B.; Liu, G.; Liashenko, A.; Piskorz, P.; Komaromi, I.; Gomperts, R.; Martin, R. L.; Fox, D. J.; Keith, T.; Al-Laham, M. A.; Peng, C. Y.; Nanayakkara, A.; Gonzalez, C.; Challacombe, M.; Gill, P. M. W.; Johnson, B. G.; Chen, W.; Wong, M. W.; Andres, J. L.; Head-Gordon, M.; Replogle, E. S.; Pople, J. A. *Gaussian 98*, revision A.9; Gaussian, Inc.: Pittsburgh, PA, 1998.

(21) Becke, A. D. *J. Chem. Phys.* **1993**, *98*, 5648.

(22) Perdew, J. P.; Burke, K.; Wang, Y. *Phys. Rev. B* **1996**, *54*, 16533.

(23) Lee, C.; Yang, W.; Parr, R. G. *Phys. Rev. B* **1988**, *37*, 785.

(24) Dunning, T. H., Jr. *J. Chem. Phys.* **1989**, *90*, 1007.

(25) Bruno, I. J.; Cole, J. C.; Edgington, P. R.; Kessler, M. K.; Macrae, C. F.; McCabe, P.; Pearson, J.; Taylor, R. *Acta Crystallogr.* **2002**, *B58*, 389.

(26) Becker, R. S.; Richey, W. F. *J. Am. Chem. Soc.* **1967**, *89*, 1298.

(27) Knyazhansky, M. I.; Metelitsa, A. V.; Kletskii, M. E.; Millov, A. A.; Besugliy, S. O. *J. Mol. Struct.* **2000**, *526*, 65.

(28) Raohatgi-Mukherjee, K. K. *Fundamentals of Photochemistry*; Wiley Eastern Limited: New Delhi, 1978.

(29) Glynn, S. P. M.; Azumi, T.; Kinoshita, M. *Molecular Spectroscopy of the Triplet State*; Prentice Hall: Englewood Clifs, New Jersey, 1969.

(30) Hohenberg, P.; Kohn, W. *Phys. Rev. B.* **1964**, *136*, 864.

(31) Lazarou, Y. G. MORIO (molecular drawing program), 2004.

(32) Lazarou, Y. G.; Prosmitis, A. V.; Papadimitriou, V. C.; Papagiannakopoulos, P. *J. Phys. Chem. A* **2001**, *105*, 6729.